ARMY RESEARCH LABORATORY

Computational Fluid Dynamics Modeling of Multi-body Missile Aerodynamic Interference

Jubaraj Sahu
Harris L. Edge
Karen R. Heavey
Earl N. Ferry

ARL-TR-1765 AUGUST 1998

Approved for public release; distribution is unlimited.

The findings in this report are not to be construed as an official Department of the Army position unless so designated by other authorized documents.

Citation of manufacturer's or trade names does not constitute an official endorsement or approval of the use thereof.

Destroy this report when it is no longer needed. Do not return it to the originator.

Army Research Laboratory
Aberdeen Proving Ground, MD 21005-5066

ARL-TR-1765

August 1998

Computational Fluid Dynamics Modeling of Multi-body Missile Aerodynamic Interference

Jubaraj Sahu
Harris L. Edge
Karen R. Heavey
Earl N. Ferry
Weapons & Materials Research Directorate

Abstract

Computational fluid dynamics (CFD) calculations have been performed for a multi-body system consisting of a main missile and a number of submunitions. Numerical flow field computations have been made for various orientations and locations of submunitions using an unsteady, zonal Navier-Stokes code and the chimera composite grid discretization technique at transonic speeds and zero degree angle of attack. Both steady state and unsteady numerical results have been obtained and compared for two submunitions and a missile system. Computed results show the details of the expected flow field features, including the shock interactions. Computed results are compared with limited experimental data obtained for the same configuration and conditions and are generally found to be in good agreement with the data. Comparison of the unsteady and steady state results shows an appreciable change in the aerodynamic forces and moments.

TABLE OF CONTENTS

INTENTIONALLY LEFT BLANK

LIST OF FIGURES

INTENTIONALLY LEFT BLANK

LIST OF TABLES

INTENTIONALLY LEFT BLANK

COMPUTATIONAL FLUID DYNAMICS MODELING OF MULTI-BODY MISSILE AERODYNAMIC INTERFERENCE

1. INTRODUCTION

Aerodynamic forces and moments are critical design parameters used in the design of artillery shells and bodies flying in relative motion to each other. The advancement of computational fluid dynamics (CFD) has had a major impact on projectile design and development.[1-4] Improved computer technology and state-of-the-art numerical procedures enable scientists to develop solutions to complex, three-dimensional problems associated with projectile and missile aerodynamics. The research effort has focused on the development and application of a versatile overset grid numerical technique to solve multi-body aerodynamic problems. This numerical capability has been used successfully to determine the aerodynamics on a multi-body problem of brilliant antiarmor (BAT) submunition dispersal from the Army tactical missile system (TACMS). Figure 1 shows a schematic diagram of this multi-body system.

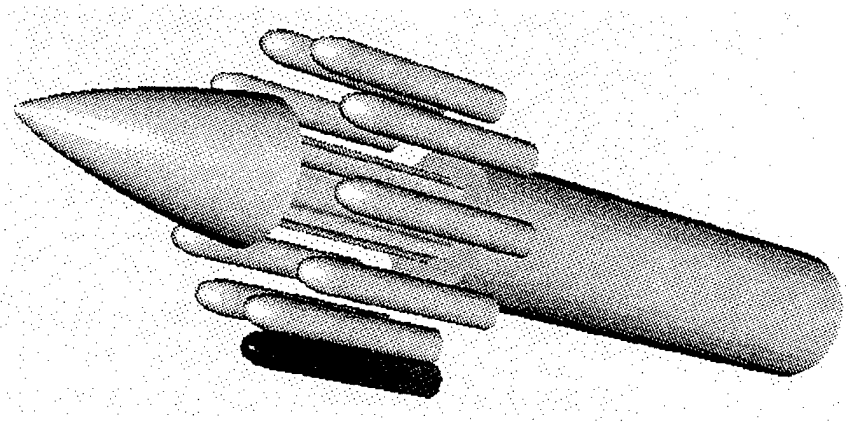

Figure 1. Schematic Diagram of Multi-body System.

The complexity and uniqueness of this type of multi-body problem result from the aerodynamic interference of the individual components, which include three-dimensional (3-D) shock-shock interactions, shock-boundary layer interactions, and highly viscous-dominated separated flow regions. The overset grid technique, which is ideally suited to this problem, involves generating numerical grids about each body component and then oversetting them onto a base grid to form the complete model. With this composite overset grid approach, it is possible to determine the 3-D interacting flow field of the multi-body system and the associated aerodynamic forces and

moments at different positions and orientations without the need for costly regridding. The solution procedure of the developed technique is to compute the interference flow field at multiple locations until final converged solutions are obtained and then to integrate the pressure and viscous forces to obtain the total forces and moments. The complex physics and fluid dynamics structure of the 3-D aerodynamic interference for this multi-body problem have been identified.

A description of the computational algorithm and the chimera technique follows. The next section describes the model geometry and various computational grids used in the numerical computations. Results are shown for both steady state computations for the missile with single and multiple BAT submunitions and a dynamic computation with two submunitions at transonic speeds.

2. SOLUTION TECHNIQUE

2.1 Governing Equations

The complete set of 3-D, time-dependent, generalized geometry, Reynolds-averaged, thin layer Navier-Stokes equations is solved numerically to obtain a solution to this problem and can be written in general spatial coordinates ξ, η, and ζ as follows:[5]

$$\partial_\tau \hat{q} + \partial_\xi \hat{F} + \partial_\eta \hat{G} + \partial_\zeta \hat{H} = Re^{-1} \partial_\zeta \hat{S}, \tag{1}$$

in which

$\xi = \xi(x, y, z, t)$ - longitudinal coordinate;
$\eta = \eta(x, y, z, t)$ - circumferential coordinate
$\zeta = \zeta(x, y, z, t)$ - nearly normal coordinate;
$\tau = t$ - time

In Equation 1, $\hat{q}$ contains the dependent variables: density, three velocity components, and energy. The thin layer approximation is used here, and the viscous terms involving velocity gradients in both the longitudinal and circumferential directions are neglected. The viscous terms are retained in the normal direction, ζ, and are collected into the vector $\hat{S}$. In the wake or the base region, similar viscous terms[1] are also added in the streamwise direction, ξ. An implicit, approximately factored scheme is used to solve these equations.

2.2 Numerical Algorithm

The implicit, approximately factored scheme for the thin layer Navier-Stokes equations using central differencing in the η and ζ directions and upwinding in ξ is written in the following form:[6]

$$\left[I + i_b h \delta_\xi^b \left(\hat{A}^+ \right)^n + i_b h \delta_\zeta \hat{C}^n - i_b h Re^{-1} \bar{\delta}_\zeta J^{-1} \hat{M}^n J - i_b D_i|_\zeta \right]$$
$$\times \left[I + i_b h \delta_\xi^f \left(\hat{A}^- \right)^n + i_b h \delta_\eta \hat{B}^n - i_b D_i|_\eta \right] \Delta \hat{Q}^n$$
$$= - i_b \Delta t \left\{ \delta_\xi^b \left[\left(\hat{F}^+ \right)^n - \hat{F}_\infty^+ \right] + \delta_\xi^f \left[\left(\hat{F}^- \right)^n - \hat{F}_\infty^- \right] + \delta_\eta \left(\hat{G}^n - \hat{G}_\infty \right) + \delta_\zeta \left(\hat{H}^n - \hat{H}_\infty \right) - Re^{-1} \bar{\delta}_\zeta \left(\hat{S}^n - \hat{S}_\infty \right) \right\}$$
$$- i_b D_e \left(\hat{Q}^n - \hat{Q}_\infty \right), \qquad (2)$$

in which h = Δt or $(\Delta t)/2$ and the free-stream base solution is used. Here, δ is typically a three-point second order accurate central difference operator, $\bar{\delta}$ is a midpoint operator used with the viscous terms, and the operators δ_ξ^b and δ_ξ^f are backward and forward three-point difference operators. The flux $\hat{F}$ has been eigensplit, and the matrices $\hat{A}$, $\hat{B}$, $\hat{C}$, and $\hat{M}$ result from local linearization of the fluxes about the previous time level. Here, J denotes the Jacobian of the coordinate transformation. Dissipation operators D_e and D_i are used in the central space differencing directions.

2.3 Chimera Scheme

The chimera overset grid technique[7–9], which is ideally suited to multi-body problems, involves generating independent grids about each body and then oversetting them onto a base grid to form the complete model. This procedure reduces a complex multi-body problem into a number of simpler subproblems. An advantage of the overset grid technique is that it allows computational grids to be obtained for each body component separately and thus makes the grid-generation process easier. Because each component grid is generated independently, portions of one grid may lie within a solid boundary contained within another grid. Such points lie outside the computational domain and are excluded from the solution process. This was achieved by modifying Equation 2 for chimera overset grids by the introduction of the flag i_b. This i_b array accommodates the possibility of having arbitrary holes in the grid. The i_b array is defined so that i_b = 1 at normal grid points and i_b = 0 at hole points. Thus, when i_b = 1, Equation 2 becomes the standard scheme, but when i_b = 0, the algorithm reduces to $\Delta \hat{Q}^n = 0$ or $\hat{Q}^{n+1} = \hat{Q}^n$, leaving $\hat{Q}$ unchanged at hole points. The set of grid points that form the border between the hole points and the normal field points are called inter-grid boundary points. These points are updated by interpolating the solution from the overset grid that created the hole. Values of the i_b array and the interpolation coefficients needed for this update are provided by a separate algorithm.[7] Figure 2 shows an example where the parent missile grid is a major grid and the BAT submunition grid is a minor grid. The submunition grid is completely overlapped by the missile grid, and thus, its outer

boundary can obtain information by interpolation from the missile grid. Similar data transfer or communication is needed from the submunition grid to the missile grid. However, a natural outer boundary that overlaps the submunition grid does not exist for the missile grid. The overset grid technique creates an artificial boundary or a hole boundary within the missile grid that provides the required path for information transfer from the submunition grid to the missile grid. The resulting hole region is excluded from the flow field solution in the missile grid.

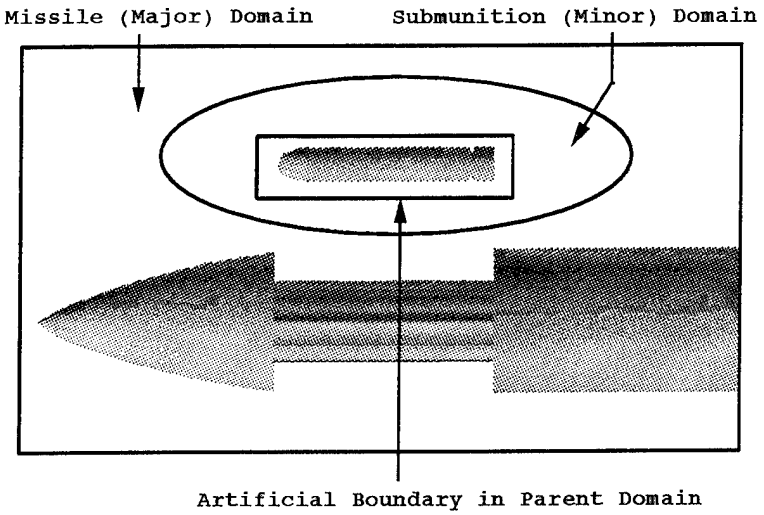

Figure 2. Inter-grid Communications.

The chimera method depends on three functions: domain connectivity, aerodynamics, and body dynamics. The aerodynamics code depends on the domain connectivity code[10] to supply hole and interpolation information. The domain connectivity code, in turn, depends on the body dynamics code to supply the location and orientation of the moving bodies relative to the primary body. Finally, the body dynamics code depends on the aerodynamics code to provide the aerodynamic forces and moments acting on the moving bodies. For moving body problems, all grids are allowed to move with 6 degrees of freedom (DOF) relative to an inertial reference frame. Accordingly, bodies can move with respect to others without the necessity of generating new grids. With this composite overset grid approach, it is thus possible to determine the aerodynamics associated with the bodies without the need for costly regridding. This also eliminates potential accuracy problems attributable to severe grid stretching used by many other techniques, such as the zonal blocked grid method commonly used in CFD.

3. MULTI-BODY PROBLEM DESCRIPTION

The TACMS-BAT multi-body problem involves the radial dispensing of several BAT submunitions (see Figure 1) at a transonic speed and thus was ideally suited for the numerical capability[11] described earlier. The 3-D radial dispensing of these submunitions depends on the initial ejection velocity. The flow field is complex and involves 3-D shock-boundary layer interactions, and TACMS-to-BAT as well as BAT-to-BAT interactions. Detailed experimental or theoretical data were not available to help evaluate the submunition dispensing phenomenon for the entire BAT system, and thus, the numerical solution of this problem was initiated. The chimera solution procedure was thus used to determine the aerodynamic interference effects, and CFD was brought into the developmental phase of the BAT program to ensure successful dispensing of the submunitions.

The missile carries 13 submunitions; the first 10 outer BAT submunitions, and then the three inner BAT submunitions, are radially dispensed from the TACMS. Once released from the missile bay, the self-guided BAT submunitions autonomously disperse over the hostile territory, use their sensors to detect targets, and deliver shaped charged warheads. The concern here is the flight dynamics and aerodynamics of the dispensing phenomenon. Application of the advanced CFD modeling technique to this multi-body dispensing problem was to provide realistic simulation, detailed understanding of the underlying aerodynamic interference effects, and design information that can lead to successfully dispensing the BAT submunitions from the TACMS.

4. MODEL GEOMETRY AND GRIDS

An advantage of the chimera technique is that it allows computational grids to be obtained for each body component separately and thus makes the grid generation process easier. Figure 3 shows a computational grid for the complete model, including the missile and the BAT submunitions. Also shown here are the sections of the three-dimensional BAT computational grids overset onto the missile grid. Figure 4 shows a computational grid for one BAT submunition. As part of the chimera procedure, this BAT grid is partially cut by the missile body itself. Similarly, the presence of the BAT submunition cuts a hole in the missile grid (see Figure 5). The missile grid consists of three zones: one on the nose region ahead of the cavity, one in the cavity itself, and the third one aft of the cavity region. Each of these three zones is a rectangular grid.

The grid around the submunition consists of two zones (one for the body and one for the base region) and was obtained using an C-topology and a rectangular topology, respectively. The

submunition grids were individually generated and then overset as shown in Figure 3 to form the complete grid system. The computational grids shown here correspond to the pitch plane. The missile grid serves as the main background grid for the computations. Figure 4 shows a computational grid for computations with the BAT submunition at a distance about a diameter away from the center line of symmetry of the missile. For steady state or unsteady dynamic computations, the same submunition grids are used, and there was no need to regenerate new submunition grids. Typically, the missile grid consisted of 983,000 points. The entire grid system consisted of about 1.2 million points for the missile and the one-BAT (with and without sting) case as well as for the two-BAT cases. Note that the grid setup allows computation of the base region flow field of the submunitions. Grid points are clustered near the missile and the BAT submunition surfaces to capture the viscous boundary layers. No attempt has been made to adapt the computational grids to gradients in the flow field variables.

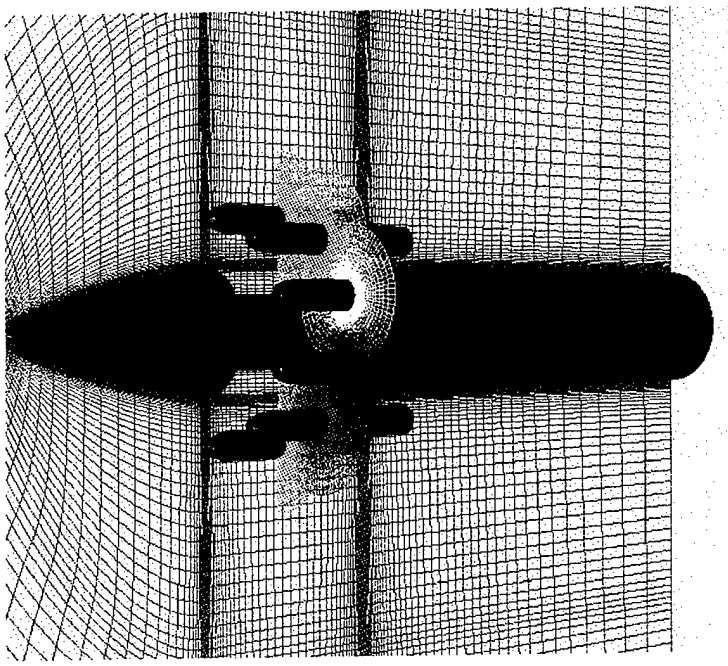

Figure 3. Grids for the BAT Submunition Dispensing From TACMS.

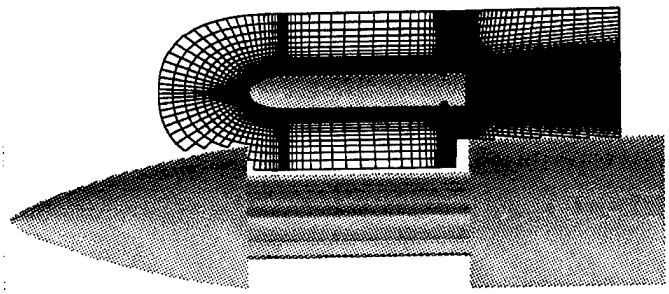

Figure 4. Computational Grids for a Submunition.

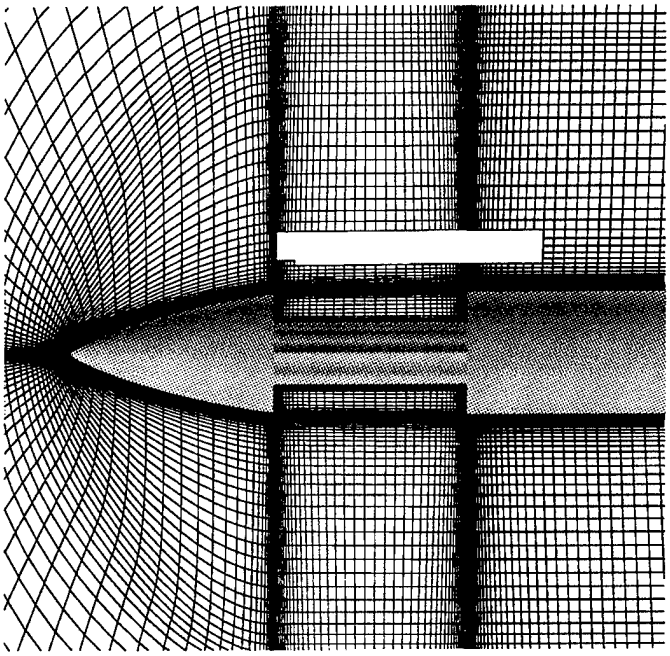

Figure 5. Computational Grids for the Missile.

The actual cavity surface of the missile bay where the BATs are stored in their original positions was used in the CFD computations. The flow field in the bay is viscously dominated, turbulent, and quite complex, with the BAT located in the near field. It is difficult to accurately determine the interference effects by theoretical or experimental means. This is especially true when the BAT is submerged in the bay. Limited wind tunnel experimental data[12] are available for a reduced scale model for the missile and BAT submunitions. However, such data can suffer from sting effects and for viscously dominated cavity flows, they may not scale to the real flight conditions.

5. RESULTS

Both steady state and a dynamic unsteady numerical calculations have been performed to numerically simulate the missile and the BAT system. Computations have been run at $M_\infty = 1.2$ and 1.5. Computational modeling is restricted to the symmetrical submunition dispersal. Here, the missile is at 0° angle of attack, and the BATs are dispensed symmetrically following the same radial trajectory away from the projectile. Appropriate symmetry is used for the one-BAT and multiple BAT cases. For the multiple BAT cases, the computational domain consists of a 36° segment in the circumferential plane (see Figure 6). Also shown is the submunition grid, which is entirely contained in the background projectile grid. Because of symmetry, the requirements for grid sizes, computer resources such as computer memory, and run time are reduced.

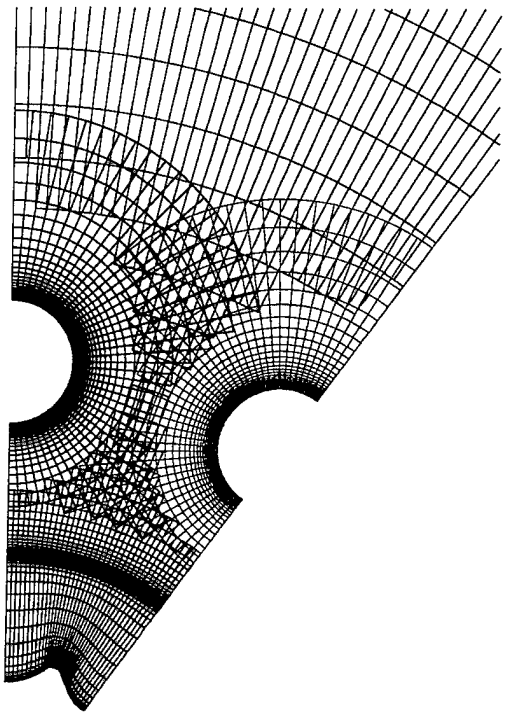

Figure 6. Circumferential Cross-Sectional Grid.

The CFD modeling was initially used to compute transonic flow over the wind tunnel model consisting of the missile and one sting-mounted BAT. Computations were also performed for the BAT without the sting for direct comparison (see Figure 7). Computed Mach contours show some influence of the sting on the solution near the aft end of the cavity. Quantitatively, the presence of a sting affects the forces and moments acting on the BAT submunition and to a lesser extent, on the missile itself. Computed surface pressures obtained from the flow field solution for the BAT submunition were compared with experimentally measured pressure on the BAT and were found to be in very good agreement for two different radial locations of the submunitions (see Figure 8). Computed surface pressure on the missile cavity surface is shown in Figure 9 for the one-BAT case. Computed surface pressures again agree well with the experimental data. These comparisons inspire confidence in the quality of the CFD results for the multi-body system consisting of the missile and one BAT. The CFD modeling includes the wake and the base region of the BAT as they would be in real flight situations.

For the actual system, which consists of the TACMS and the 10 outer BAT submunitions, the present CFD capability was then used to compute the flow field for the flight conditions. This case now included not only BAT-to-TACMS interactions but also 3-D BAT-to-BAT interactions. Figure 10 shows the results of such a numerical simulation for the symmetrical dispensation of all 10 BAT submunitions from the TACMS. The computed Mach contours are shown at two selected positions along the BAT submunitions. The 3-D BAT-to-BAT interactions are clearly depicted in this figure. To promote better understanding of the aerodynamic interference associated with the TACMS-BAT system, numerical computations were performed with the BAT submunitions at various radial positions away from the missile. Figure 11 shows the computed results for these cases for the actual transonic flight conditions from bottom to top. The first position corresponds to the BAT submunitions semi-chambered in the bay (cavity) of the missile. The next two positions are approximately 20.4 and 25.8 inches away from the centerline of the missile. These pictures clearly show the complicated aerodynamic interference between the missile and the BAT submunitions in a longitudinal view. The flow inside the cavity is primarily subsonic and contains large regions of separated flow. The dramatic change in the interacting flow field can be observed as the BAT submunitions move farther and farther radially out from the semi-chambered position. The flow field over the submunitions is 3-D, and the computed results clearly show this feature in the wake or base region of the submunitions.

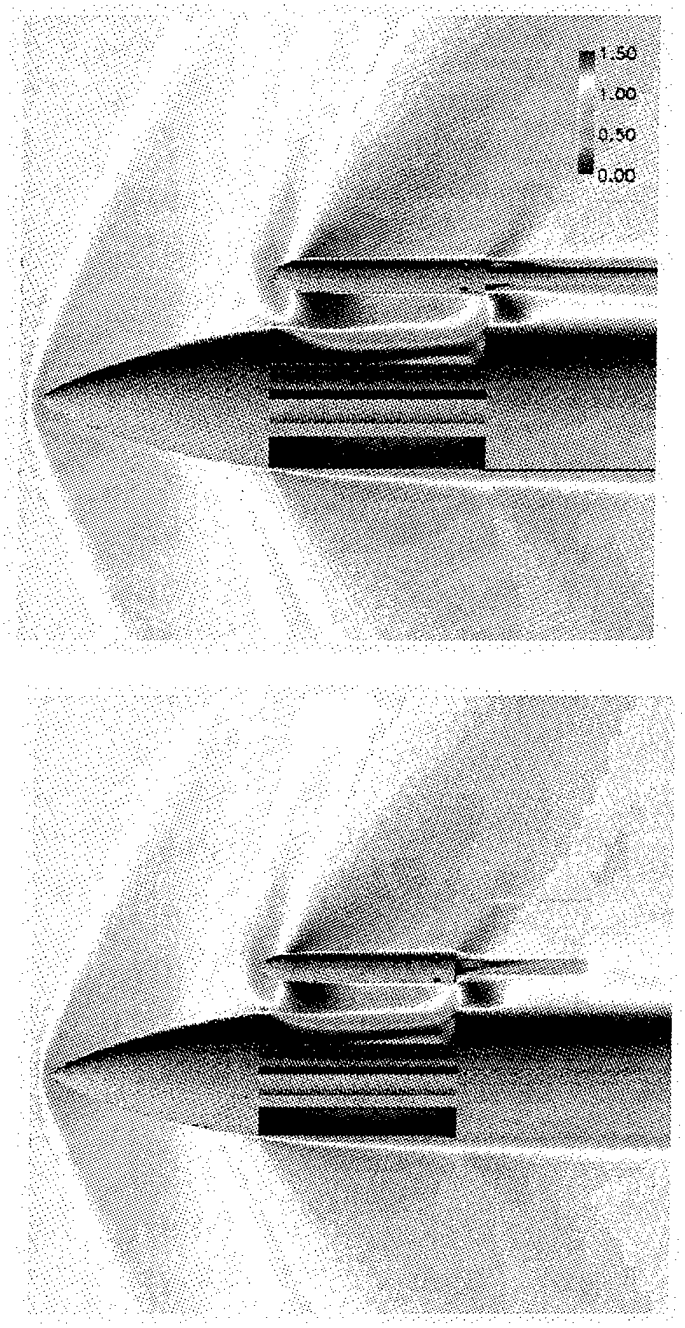

Figure 7. Computed Mach Contours for a Single Submunition With Sting and No Sting.

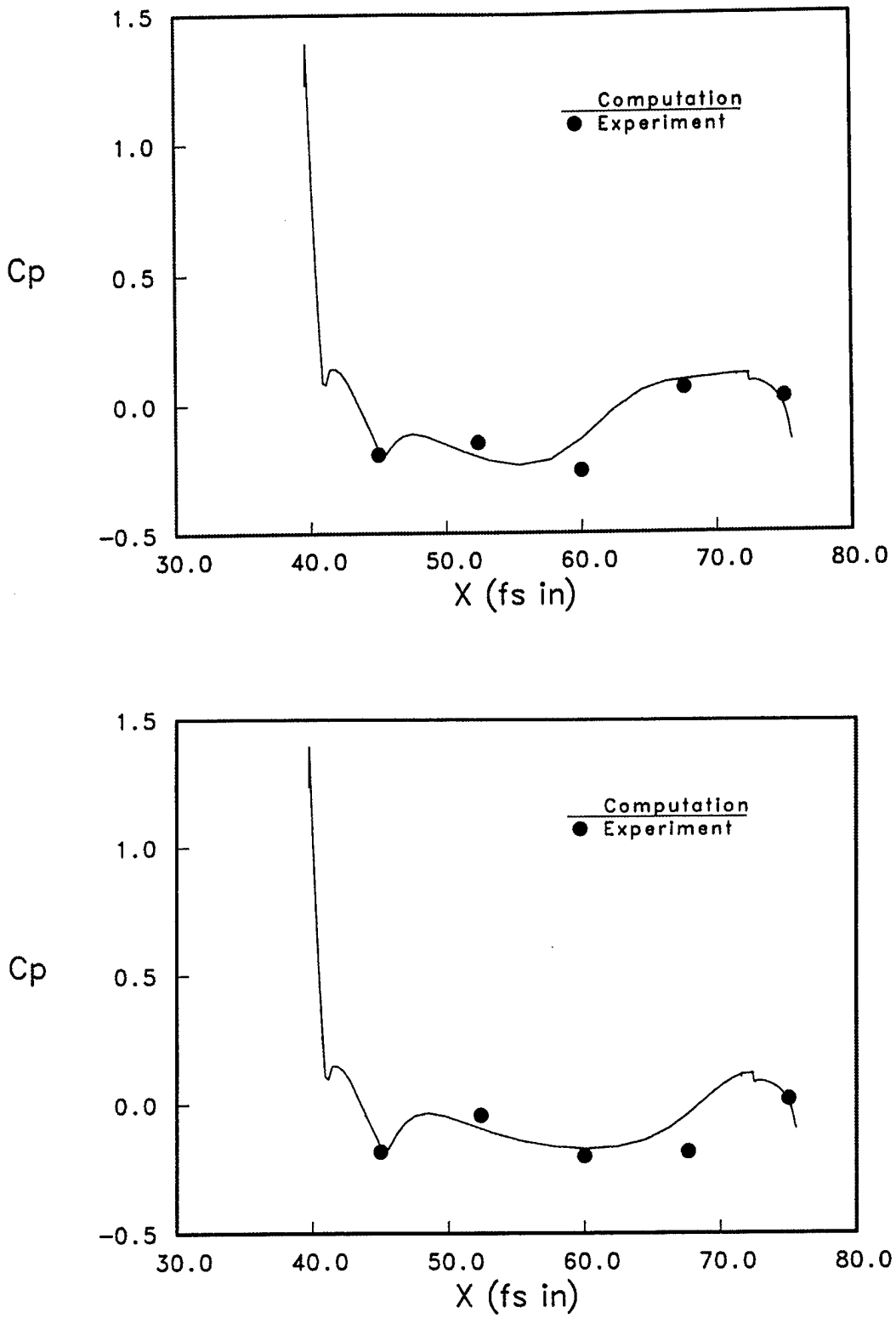

Figure 8. Computed Surface Pressures on the Submunition at Radius 20.35 (top) and 25.85 inches (bottom).

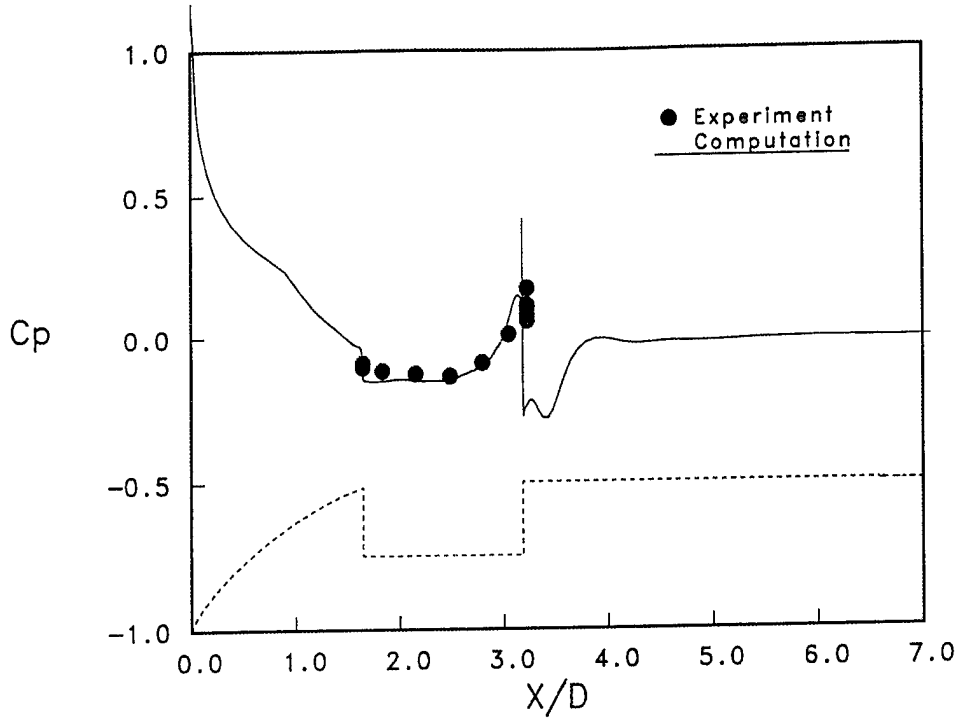

Figure 9. Computed Surface Pressure on the Missile.

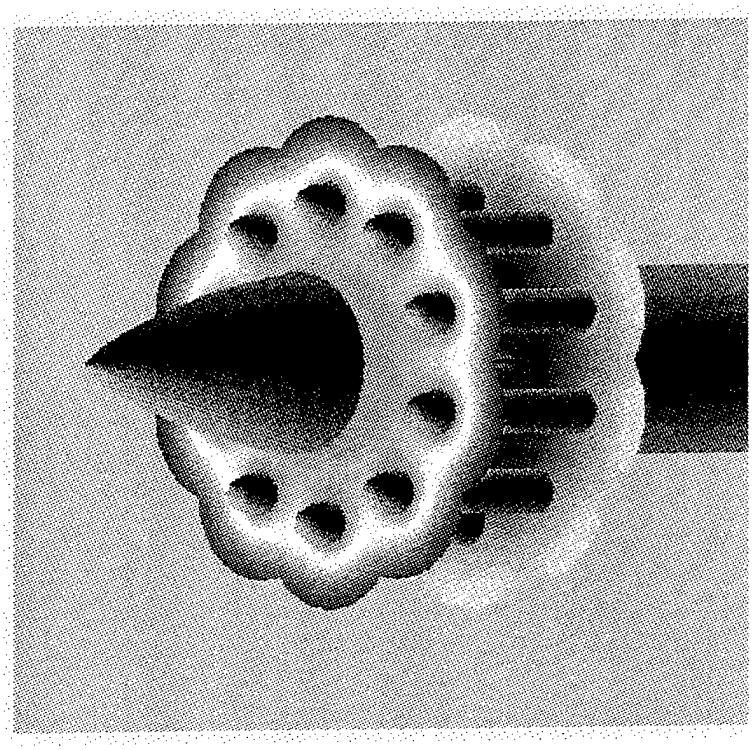

Figure 10. BAT-to-BAT Interaction.

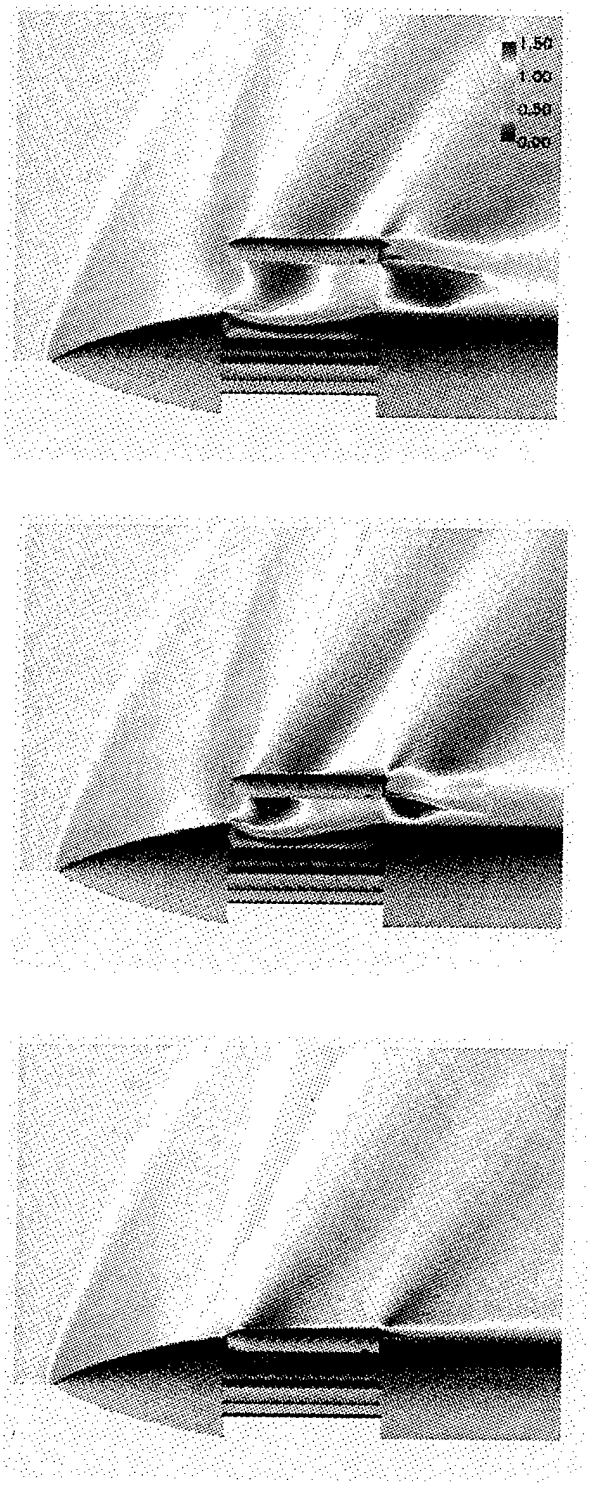

Figure 11. BAT-to-TACMS Interaction for Various Submunition Locations.

Computations were also performed for this multi-body problem with five BATs at M_∞ = 1.2 and $\alpha = 0°$. This case included modeling of half of the actual missile bay. Because of symmetry, CFD modeling uses four side BATs and a half BAT on the top (lee side) as well as the bottom (wind side). Figure 12 shows the Mach number contours for this case. Qualitatively, it shows the expected shock structure and the flow field resulting from the submunition interactions. Figures 13 and 14 show the circumferential Mach number contours for the five-BAT case at two longitudinal stations, 2.5 and 3.2 calibers from the nose of the missile. Both locations are in the cavity of the missile. These figures show the BAT-to-BAT interactions and the effect of the cavity shape on the solutions. Figure 13 indicates a smaller region of low speed flow between the cavity surface and the bottom surfaces of the BATs and high speed flow near the top surfaces of the BATs. At a station down stream in the cavity, Figure 14 shows a large region of the low speed flow between the BATs and missile cavity surface as well as near and away from the top surfaces of the BATs. Aerodynamic forces and moments were obtained from the computed solutions. Figure 15 shows normal force coefficient, axial force coefficient, and pitching moment for the submunitions as a function of radius (measured from the centerline of the missile). These computed force (CN, CA) and moment (CM) coefficients were compared with the experimental data and are found to be in good agreement with the data. The measured axial force coefficient, CA, does not include base drag and computed axial force coefficient also excludes base drag of the submunitions for direct comparison.

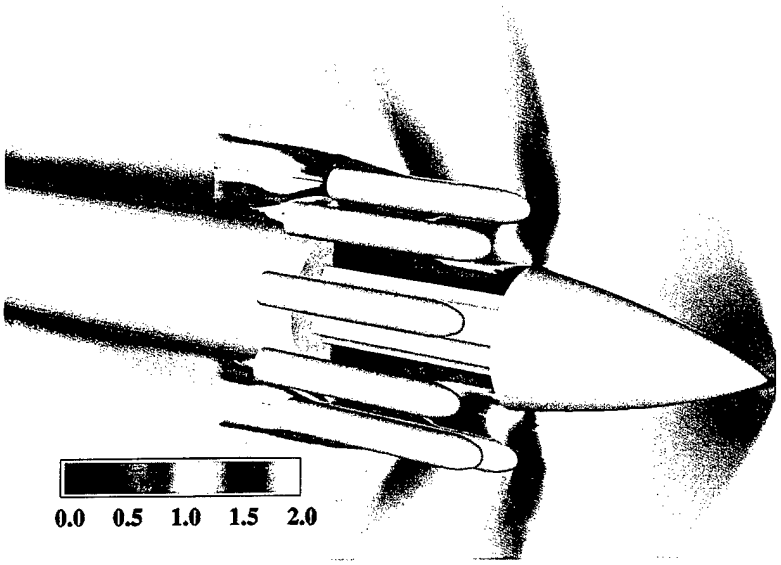

Figure 12. Mach Contours for the Five-BAT Case.

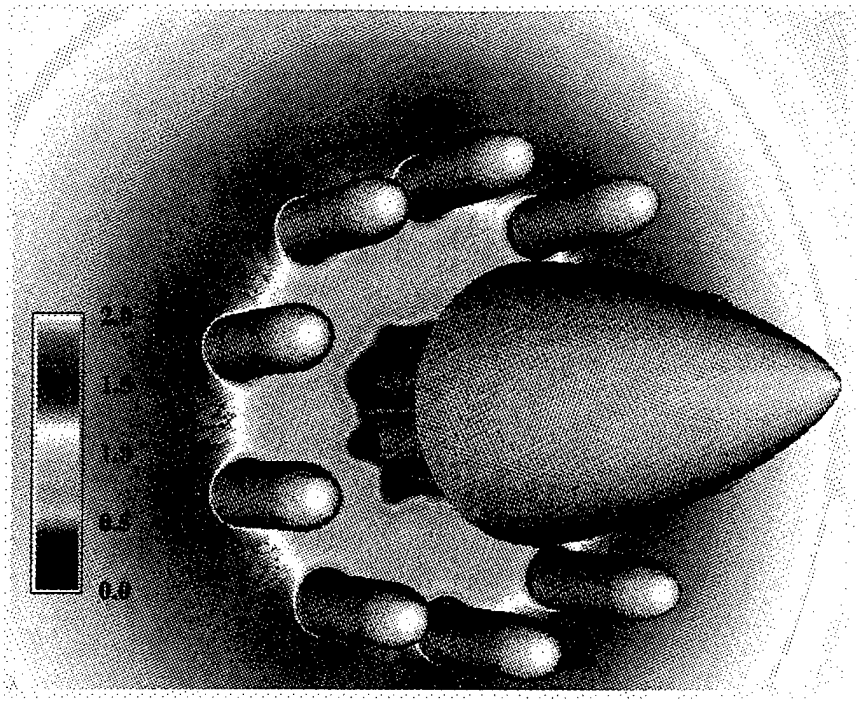

Figure 13. Mach Contours at X/D = 2.5 Calibers.

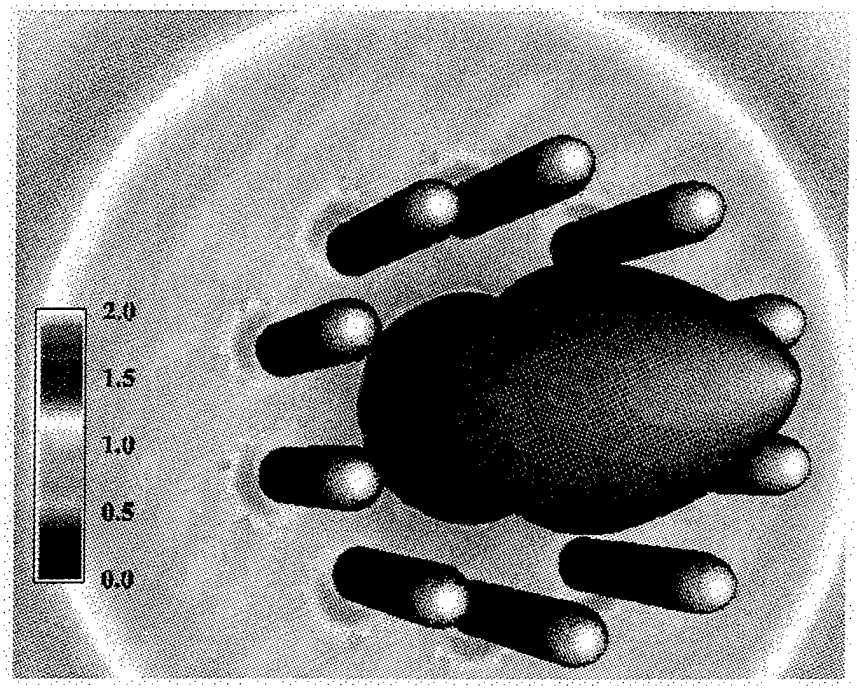

Figure 14. Mach Contours X/D = 3.2 Calibers.

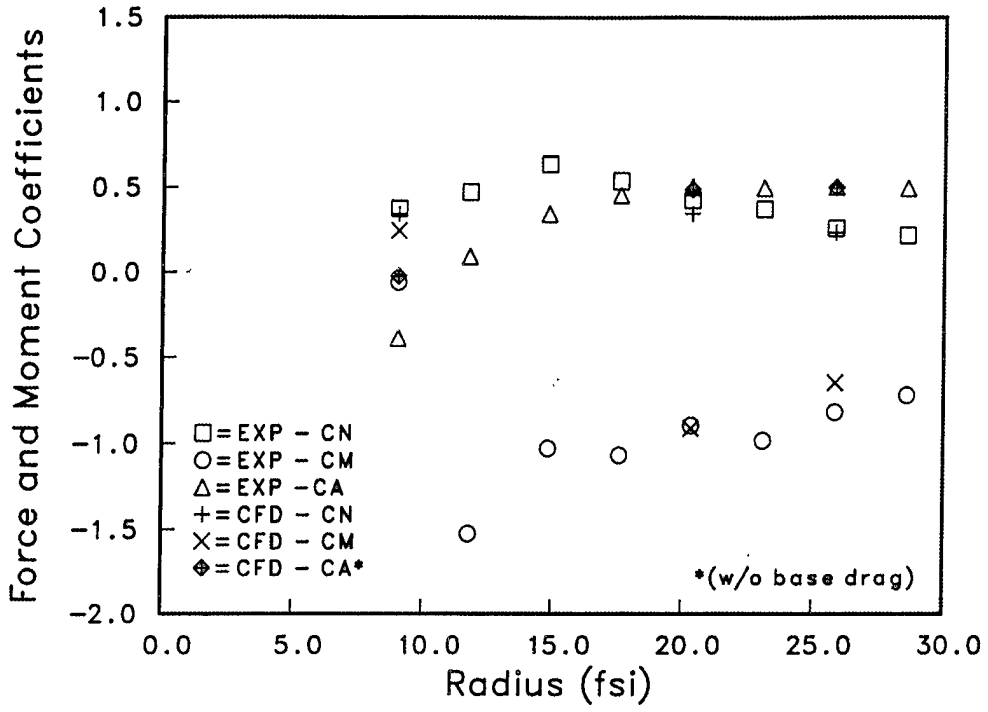

Figure 15. Force and Moment Coefficients.

A dynamic simulation was performed for the missile and the two-BAT case at $M_\infty = 1.5$ and $\alpha = 0°$. The dynamic computations were started from a converged steady state solution with the submunitions located in the cavity chamber. The same computational grids (see Figure 6) were used for the entire dynamic simulation event without the need of regridding. The chimera procedure described earlier was also used for this computation. The forces and moments provided by the aerodynamics code were used by the body dynamics code to determine the location and orientation of the moving submunitions relative to the missile. This required domain connectivity (hole and interpolation information) at each time step. The domain connectivity information was then used in the aerodynamics code to provide the aerodynamic forces and moments. This procedure was repeated at each time step during the dynamic simulation. Figure 16 shows three snapshots of computed pressure contours in time. It shows the flow field changing significantly with the submunition being dispensed. The bottom picture corresponds to the initial position of the submunitions. The other two correspond to 16 and 45 msec in time. The submunitions were restricted to the pitch plane and were not allowed to yaw or roll.

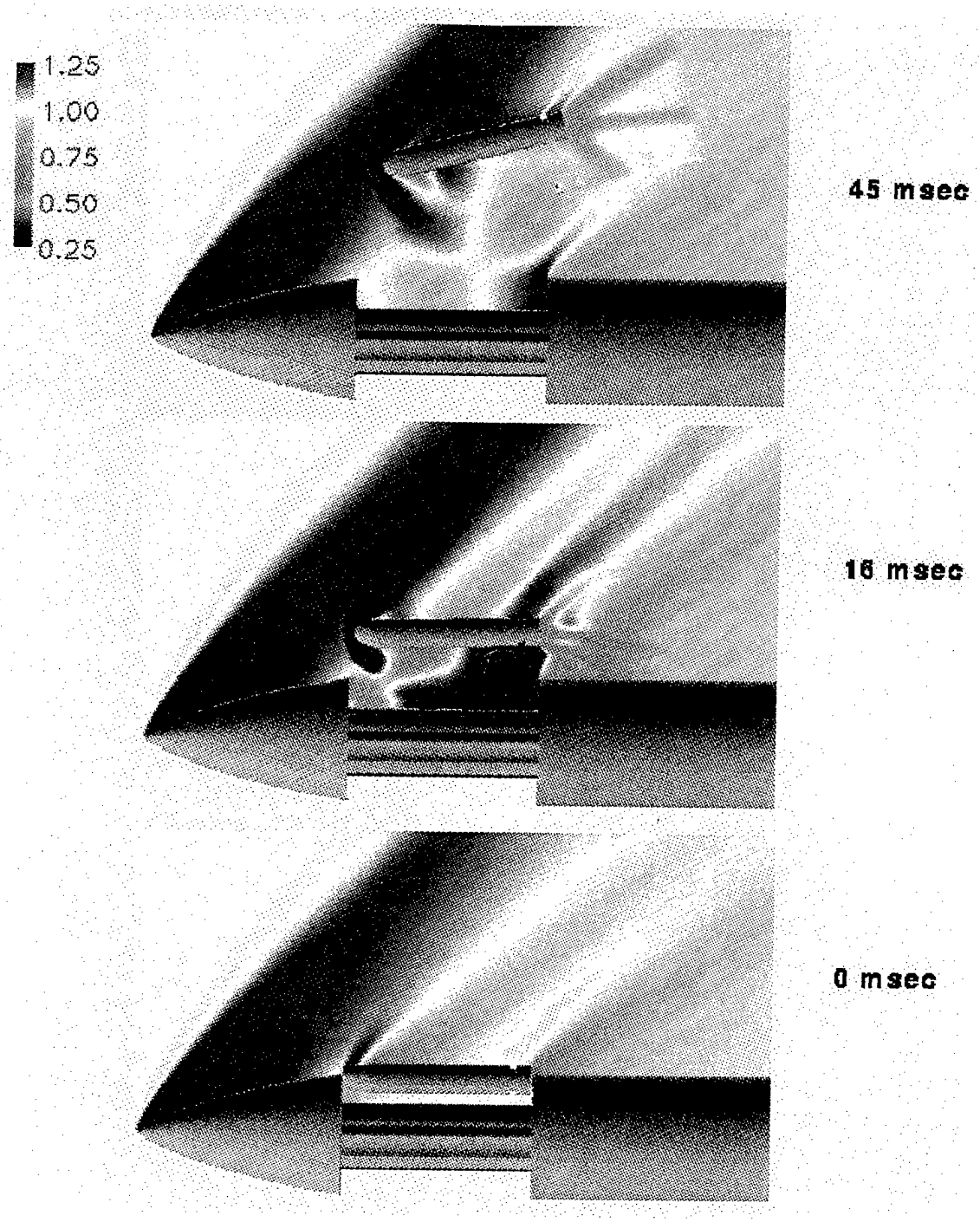

Figure 16. Mach Contours for the Dynamic Case.

Figure 17 shows the force and moment history as a function of time. Shown here are the normal force, CN, axial force, CA, and pitching moment, CM, coefficients for the submunition. Since the computations include two BAT submunitions, BAT-to-BAT interactions are included. These interactions are critical and have a strong effect on the aerodynamic forces and moments. The normal force and pitching moment coefficients indicate the unsteady nature of the interacting flow field. A case that corresponds to 16 msec in time during the dynamic simulation was selected and frozen to run a steady state computation. This case corresponded to the submunition being at an angle -1° nose down (pitch angle). A static converged solution was then obtained for the missile and the submunitions in that orientation. Comparison of the static and dynamic results for this case is shown in Table 1. Again, all three force and moment coefficients are included. The axial force coefficient (with or without base drag) does not change appreciably; however, normal force and pitching moment coefficients are seen to change significantly. These results indicate the importance of the dynamic numerical simulation, which may be needed to accurately predict the aerodynamics of the submunition dispersal.

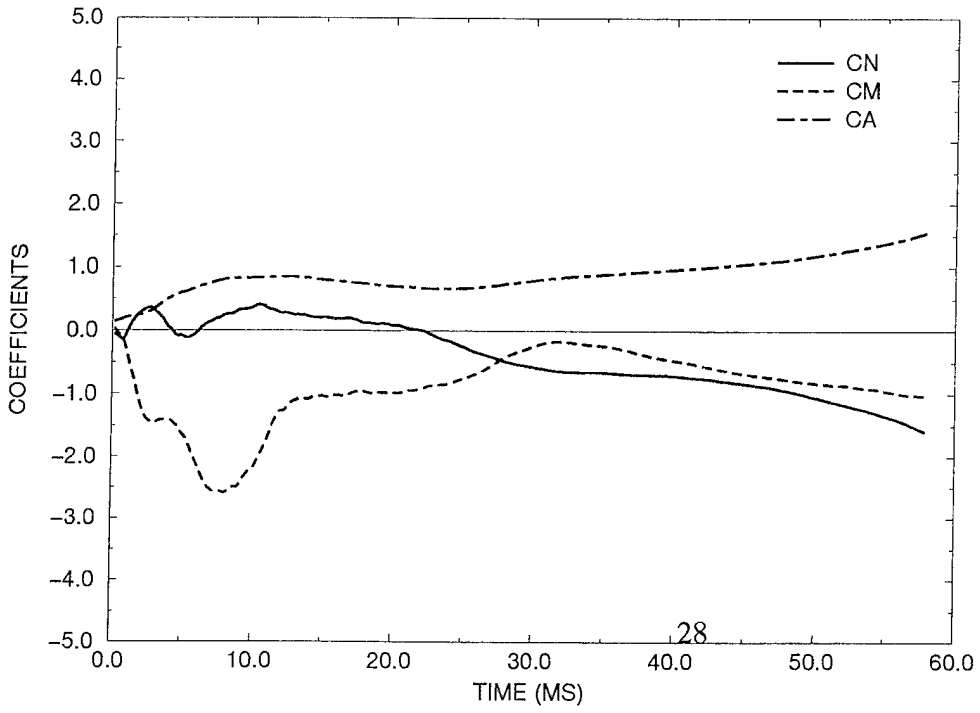

Figure 17. Time History of Force and Moment.

Table 1

Static and Dynamic Force and Moment Comparison

	DYNAMIC R = 20.23 fsi	STATIC R = 20.23 fsi
C_N	+ 0.187	+0.393
C_m	- 1.026	- 0.790
C_A		
w/base drag	+ 0.776	+ 0.794
w/o base drag	+ 0.560	+ 0.586

6. CONCLUDING REMARKS

A computational study was undertaken to compute the 3-D flow fields for a multi-body system consisting of a missile and multiple BAT submunitions. Flow computations were performed at transonic speeds (M_∞ = 1.2, 1.5) and $\alpha = 0.0°$ using a 3-D unsteady Navier-Stokes code and chimera composite grid discretization technique. Overset body-conforming grids were used to individually model the missile and the BAT submunitions. Computed results have been obtained for different locations of the submunitions. Computed pressure and Mach contours show the details of the 3-D aerodynamic interference flow field for the missile and the submunitions. The computed flow field includes both the missile-to-BAT as well as BAT-to-BAT interactions. Both computed results for sting-mounted and no-sting models have been obtained for the one-BAT case, and the computed results do not show appreciable change in the surface pressures. Computed results for the multiple BAT cases include BAT-to-BAT interactions and show their large effect on the computed forces and moments. Computed surface pressures as well as forces and moments have been compared with the experimental results for the same configuration and conditions and are generally in good agreement with the data. Dynamic unsteady results were also obtained for a multiple BAT case and compared with the static results for the same location and orientation of the submunitions. These comparisons show, in some cases, large changes in the aerodynamic force and moments between the static and dynamic computations. Future study will include modeling of asymmetrical submunition dispersal, which will require full 3-D computations and large computing resources.

This work represents the application of a chimera overlapping grids approach for accurate numerical calculation of aerodynamics involving multiple bodies with and without relative motion. The predictive numerical capability has been used to provide the development community numerical data and basic flow field design information to more effectively guide the design of a multi-body missile configuration. It allows accurate and realistic numerical prediction of interference effects and aerodynamics required for the improved design and modification of current and future multi-body missile and projectile configurations.

7. REFERENCES

1. Sahu, J., "Numerical Simulations of Transonic Flows." *International Journal for Numerical Methods in Fluids*, vol. 10, no. 8, pp. 855-873, 1990.

2. Ferry, E.N., J. Sahu, and K.R. Heavey, "Navier-Stokes Computations of Sabot Discard using Chimera Scheme." Proceedings of the 16th International Symposium on Ballistics, September 1996.

3. Sahu, J., K.R. Heavey, and E. N. Ferry, "Computational Fluid Dynamics for Multiple Projectile Configurations." Proceedings of the 3rd Overset Composite Grid and Solution Technology Symposium, Los Alamos, NM, October 1996.

4. Sahu, J., K.R. Heavey, and C. J. Nietubicz, "Time-Dependent Navier-Stokes Computations for Submunitions in Relative Motion." Proceedings of the 6th International Symposium on Computational Fluid Dynamics, Lake Tahoe, NV, Sep. 1995.

5. Pulliam, T.H., and J. L. Steger,"On Implicit Finite-Difference Simulations of Three-Dimensional Flow," *AIAA Journal*, vol. 18, no. 2, Feb. 1982, pp. 159–167.

6. Steger, J.L., S. X. Ying, and L. B. Schiff, "A Partially Flux-Split Algorithm for Numerical Simulation of Compressible Inviscid and Viscous Flows." Proceedings of the Workshop on CFD, Institute of Nonlinear Sciences, University of California, Davis, CA, 1986.

7. Steger, J.L., F. C. Dougherty, and J. A. Benek, "A Chimera Grid Scheme." *Advances in Grid Generation*, edited by K. N. Ghia and U. Ghia, ASME FED-5, June 1983.

8. Benek, J.A., T. L. Donegan, and N. E. Suhs, "Extended Chimera Grid Embedding Scheme With Application to Viscous Flows." AIAA Paper No. 87-1126-CP, 1987.

9. Meakin, R.L., "Computations of the Unsteady Flow About a Generic Wing/Pylon/Finned-Store Configuration." AIAA 92-4568-CP, August 1992.

10. Meakin, R.L., "A New Method for Establishing Inter-Grid Communication Among Systems of Overset Grids," AIAA 10th Computational Fluid Dynamics Conference, AIAA Paper No. 91-1586, June 1991.

11. Sahu, J., and C.J. Nietubicz, "Application of Chimera Technique to Projectiles in Relative Motion." ARL-TR-590, U.S. Army Research Laboratory, Aberdeen Proving Ground, MD, October 1994 (also see *AIAA Journal of Spacecraft and Rockets*, vol. 32, no. 5, Sep–Oct 1995).

12. Wooden, P.A., Brooks, W.B., Sahu, J., "Calibrating CFD predictions For Use In Multiple Store Separation Analysis," AIAA Paper No. 98-0754, January 1998.

INTENTIONALLY LEFT BLANK

NO. OF COPIES	ORGANIZATION
2	ADMINISTRATOR DEFENSE TECHNICAL INFO CENTER ATTN DTIC DDA 8725 JOHN J KINGMAN RD STE 0944 FT BELVOIR VA 22060-6218
1	DIRECTOR US ARMY RESEARCH LABORATORY ATTN AMSRL CS AL TA RECORDS MANAGEMENT 2800 POWDER MILL RD ADELPHI MD 20783-1197
1	DIRECTOR US ARMY RESEARCH LABORATORY ATTN AMSRL CI LL TECHNICAL LIBRARY 2800 POWDER MILL RD ADELPHI MD 207830-1197
1	DIRECTOR US ARMY RESEARCH LABORATORY ATTN AMSRL CS AL TP TECH PUBLISHING BRANCH 2800 POWDER MILL RD ADELPHI MD 20783-1197
7	CDR US ARMY ARDEC ATTN AMSTE AET A R DEKLEINE C NG R BOTTICELLI H HUDGINS J GRAU S KAHN W KOENIG PICATINNY ARSENAL NJ 07806-5001
1	CDR US ARMY ARDEC ATTN AMSTE CCH V PAUL VALENTI PICATINNY ARSENAL NJ 07806-5001
1	CDR US ARMY ARDEC ATTN SFAE FAS SD MIKE DEVINE PICATINNY ARSENAL NJ 07806-5001
2	USAF WRIGHT AERONAUTICAL LABS ATTN AFWAL FIMG DR J SHANG MR N E SCAGGS WPAFB OH 45433-6553
3	AIR FORCE ARMAMENT LAB ATTN AFATL/FXA STEPHEN C KORN BRUCE SIMPSON DAVE BELK EGLIN AIR FORCE BASE FL 32542-5434

NO. OF COPIES	ORGANIZATION
1	CDR NSWC CODE B40 DR W YANTA DAHLGREN VA 22448-5100
1	CDR NSWC CODE 420 DR A WARDLAW INDIAN HEAD MD 20640-5035
1	CDR NSWC ATTN DR F MOORE DAHLGREN VA 22448
1	NAVAL AIR WARFARE CENTER ATTN DAVID FINDLAY MS 3 BLDG 2187 PATUXENT RIVER MD 20670
4	DIR NASA LANGLEY RESEARCH CENTER ATTN TECH LIBRARY MR D M BUSHNELL DR M J HEMSCH DR J SOUTH LANGLEY STATION HAMPTON VA 23665
2	ARPA ATTN DR P KEMMEY DR JAMES RICHARDSON 3701 NORTH FAIRFAX DR ARLINGTON VA 22203-1714
7	DIR NASA AMES RESEARCH CENTER MS 227 8 L SCHIFF MS 258 1 T HOLST MS 258 1 D CHAUSSEE MS 258 1 M RAI MS 258 1 P KUTLER MS 258 1 P BUNING MS 258 1 B MEAKIN MOFFETT FIELD CA 94035
2	USMA DEPT OF MECHANICS ATTN LTC ANDREW L DULL M COSTELLO WEST POINT NY 10996
2	UNIV OF CALIFORNIA DAVIS DEPT OF MECHANICAL ENGRG ATTN PROF H A DWYER PROF M HAFEZ DAVIS CA 95616

NO. OF COPIES	ORGANIZATION
1	AEROJET ELECTRONICS PLANT ATTN DANIEL W PILLASCH B170 DEPT 5311 PO BOX 296 1100 WEST HOLLYVALE STREET AZUSA CA 91702
1	MIT TECH LIBRARY 77 MASSACHUSETTS AVE CAMBRIDGE MA 02139
1	GRUMANN AEROSPACE CORP AEROPHYSICS RESEARCH DEPT ATTN DR R E MELNIK BETHPAGE NY 11714
2	MICRO CRAFT INC ATTN DR JOHN BENEK NORMAN SUHS 207 BIG SPRINGS AVE TULLAHOMA TN 37388-0370
1	LANL ATTN MR BILL HOGAN MS G770 LOS ALAMOS NM 87545
1	METACOMP TECHNOLOGIES INC ATTN S R CHAKRAVARTHY 650 S WESTLAKE BLVD SUITE 200 WESTLAKE VILLAGE CA 91362-3804
2	ROCKWELL SCIENCE CENTER ATTN S V RAMAKRISHNAN V V SHANKAR 1049 CAMINO DOS RIOS THOUSAND OAKS CA 91360
1	ADVANCED TECHNOLOGY CTR ARVIN/CALSPAN AERODYNAMICS RESEARCH DEPT ATTN DR M S HOLDEN PO BOX 400 BUFFALO NY 14225
1	UNIV OF ILLINOIS AT URBANA CHAMPAIGN DEPT OF MECH & IND ENGINEERING ATTN DR J C DUTTON URBANA IL 61801
1	UNIVERSITY OF MARYLAND DEPT OF AEROSPACE ENGRG ATTN DR J D ANDERSON JR COLLEGE PARK MD 20742
1	UNIVERSITY OF NOTRE DAME DEPT OF AERONAUTICAL & MECH ENGRG ATTN PROF T J MUELLER NOTRE DAME IN 46556
1	UNIVERSITY OF TEXAS DEPT OF AEROSPACE ENGRG MECH ATTN DR D S DOLLING AUSTIN TX 78712-1055
1	UNIVERSITY OF DELAWARE DEPT OF MECHANICAL ENGRG ATTN DR JOHN MEAKIN NEWARK DE 19716
4	COMMANDER USAAMCOM ATTN AMSAM RD SS AT ERIC KREEGER GEORGE LANDINGHAM CLARK D MIKKELSEN ED VAUGHN REDSTONE ARSENAL AL 35898-5252
4	LOCKHEED MARTIN VOUGHT SYSTEMS PO BOX 650003 M/S EM 55 ATTN PERRY WOODEN W B BROOKS JENNIE FOX ED MCQUILLEN DALLAS TX 75265-0003
1	COMMANDER US ARMY TACOM-ARDEC BLDG 162S ATTN AMCPM DS MO PETER J BURKE PICATINNY ARSENAL NJ 07806-5000
	ABERDEEN PROVING GROUND
2	DIRECTOR US ARMY RESEARCH LABORATORY ATTN AMSRL CI LP (TECH LIB) BLDG 305 APG AA
2	CDR US ARMY ARDEC FIRING TABLES ATTN R LIESKE R EITMILLER BLDG 120

NO. OF COPIES	ORGANIZATION
31	DIR USARL
	ATTN AMSRL WM B A HORST
	E SCHMIDT
	AMSRL WM BC P PLOSTINS
	D LYON J GARNER
	M BUNDY H EDGE
	B GUIDOS K HEAVEY
	V OSKAY A MIKHAIL
	J SAHU P WEINACHT
	S WILKERSON
	AMSRL ST J ROCCHIO
	AMSRL WM BA F BRANDON
	T BROWN W D'AMICO
	B DAVIS E FERGUSON
	M HOLLIS
	AMSRL WM BB C SHOEMAKER
	AMSRL WM BD B FORCH
	AMSRL WM BE G WREN
	M NUSCA
	AMSRL WM BF J LACETERA
	AMSRL WM TB R LOTTERO
	AMSRL CI H C NIETUBICZ
	AMSRL CI HC D HISLEY
	D PRESSEL W STUREK

INTENTIONALLY LEFT BLANK

REPORT DOCUMENTATION PAGE

Form Approved OMB No. 0704-0188

1. AGENCY USE ONLY *(Leave blank)*	2. REPORT DATE	3. REPORT TYPE AND DATES COVERED
	August 1998	Final

4. TITLE AND SUBTITLE

Computational Fluid Dynamics Modeling of Multi-body Missile Aerodynamic Interference

5. FUNDING NUMBERS

PR: 1L162618AH80

6. AUTHOR(S)

Sahu, J.; Edge, H.L.; Heavey, K.R.; Ferry, E.N. (all of ARL)

7. PERFORMING ORGANIZATION NAME(S) AND ADDRESS(ES)

U.S. Army Research Laboratory
Weapons & Materials Research Directorate
Aberdeen Proving Ground, MD 21010-5066

8. PERFORMING ORGANIZATION REPORT NUMBER

9. SPONSORING/MONITORING AGENCY NAME(S) AND ADDRESS(ES)

U.S. Army Research Laboratory
Weapons & Materials Research Directorate
Aberdeen Proving Ground, MD 21010-5066

10. SPONSORING/MONITORING AGENCY REPORT NUMBER

ARL-TR-1765

11. SUPPLEMENTARY NOTES

12a. DISTRIBUTION/AVAILABILITY STATEMENT

Approved for public release; distribution is unlimited.

12b. DISTRIBUTION CODE

13. ABSTRACT *(Maximum 200 words)*

Computational fluid dynamics (CFD) calculations have been performed for a multi-body system consisting of a main missile and a number of submunitions. Numerical flow field computations have been made for various orientations and locations of submunitions using an unsteady, zonal Navier-Stokes code and the chimera composite grid discretization technique at transonic speeds and zero degree angle of attack. Both steady state and unsteady numerical results have been obtained and compared for two submunitions and a missile system. Computed results show the details of the expected flow field features, including the shock interactions. Computed results are compared with limited experimental data obtained for the same configuration and conditions and are generally found to be in good agreement with the data. Comparison of the unsteady and steady state results shows an appreciable change in the aerodynamic forces and moments.

14. SUBJECT TERMS

chimera technique
computational fluid dynamics
missile interference
multiple body

15. NUMBER OF PAGES

35

16. PRICE CODE

17. SECURITY CLASSIFICATION OF REPORT	18. SECURITY CLASSIFICATION OF THIS PAGE	19. SECURITY CLASSIFICATION OF ABSTRACT	20. LIMITATION OF ABSTRACT
Unclassified	Unclassified	Unclassified	